Synthesis and in Vitro Evaluation of a Rhenium-Cyclized Somatostatin Derivative Series

Heather M. Bigott-Hennkens,[†,‡,§] Sulochana Junnotula,[§] Lixin Ma,[△,⊥,#,○] Fabio Gallazzi,[▽] Michael R. Lewis,*[,‡,△,#,○] and Silvia S. Jurisson*[,§,△,#]

Life Sciences Fellowships Program, Department of Veterinary Medicine and Surgery, Department of Chemistry, Department of Radiology, International Institute of Nano and Molecular Medicine, Nuclear Science and Engineering Institute, and Structural Biology Core, University of Missouri—Columbia, Columbia, Missouri 65211, and Research Service, Harry S. Truman Memorial Veterans' Hospital, Columbia, Missouri 65201

Received August 27, 2007

The structure–activity relationships of a series of rhenium (Re)-cyclized octreotide derivatives are described. The effects of changes in the peptide sequence, *N*-terminus, and *C*-terminus on metal cyclization, as well as binding to the somatostatin receptor, were investigated. Each peptide complex was found to have an integrated Re(V) core with a single metal oxo group, two coordination sites filled by the cysteine sulfhydryls, and another by the amide nitrogen of Phe^3/Tyr^3. The final coordination site was determined by the peptide *N*-terminus: the *N*-terminal amine coordinated for *N*-NH_2 peptides and the amide nitrogen of Thr^6 for peptides with acetylated *N*-termini. Re-cyclization of the octreotide derivatives led to structural perturbations of the somatostatin receptor-binding sequence relative to the Re—free disulfide analogues, resulting in reduced binding affinities. The findings presented herein demonstrate the importance of understanding the consequences of structural modifications when designing metal—peptide complexes for somatostatin receptor targeting.

Introduction

Radiolabeled antibodies, peptides, and small molecules can be used for selective targeting of antigens and receptors on tumor cells, enabling highly specific molecular imaging and radiotherapy of cancer. For example, somatostatin (somatotropin release-inhibiting factor or SRIF) receptor-expressing tumors have received considerable attention following the FDA approval of an ^{111}In-labeled somatostatin derivative (^{111}In-DTPA-D-Phe-c(Cys-Phe-D-Trp-Lys-Thr-Cys)-Thr(ol), ^{111}In-DTPA-octreotide) for the diagnosis of pancreatic, carcinoid, lung, and other cancers that express somatostatin receptors (SSTR) on their cell surfaces. Like ^{111}In-DTPA-octreotide, most of the work reported to date with radiolabeled SRIF analogues has employed a bifunctional chelate (BFC) approach, in which a radiometal chelating moiety (e.g., DTPA for ^{111}In, DOTA for ^{90}Y/^{177}Lu, EDDA/HYNIC for ^{99m}Tc) is appended to the receptor-targeting peptide.[1–11] Octreotide, an eight amino acid peptide cyclized by a disulfide bond between the two Cys residues (D-Phe-c(Cys-**Phe-D-Trp-Lys-Thr**-Cys)-Thr(ol); SSTR binding sequence in bold), and its derivatives are frequently radiolabeled with this approach, due to their stability in vivo and high SSTR[a] affinity.

The lead compounds arising from such studies have demonstrated excellent imaging characteristics and/or promise for peptide receptor radionuclide therapy (PRRT), albeit with certain drawbacks. Van Essen et al. give a comprehensive summary of the efficacies and limitations of three radiolabeled SRIF analogues used in PRRT: ^{111}In-DTPA-octreotide (negligible toxicity, but low incidence of objective responses), ^{90}Y-DOTA-Tyr^3-octreotide (substantial response rates, yet caused nephrotoxicity), and ^{177}Lu-DOTA-Tyr^3-octreotate (significant response rates and lower toxicity, but may not be effective in large tumors).[1] With another promising radiolabeled SRIF analogue, ^{99m}Tc-EDDA/HYNIC-Tyr^3-octreotide, nonspecific uptake in the bowel and inflammatory lesions led to false-positive results, requiring additional scanning after injection and creating potential patient compliance complications.[10,11] While these agents have shown promise for use in clinical imaging and targeted radiotherapy, the development of superior radiolabeled SRIF analogues, with higher response rates, lower nontarget tissue uptake and toxicity, and rapid clearance from excretion organs, is still warranted.

Introducing a radiometal into a somatostatin analogue as an integral part of the peptide molecule is an alternative to the BFC-radiolabeling approach. Developing Tc agents for imaging somatostatin receptors with single photon emission computed tomography (SPECT) is attractive due to the advantage of potential translation to ^{186}Re/^{188}Re (rhenium-186/188) analogues

* To whom correspondence should be addressed. (S.S.J.) Phone: (573) 882-2107. Fax: (573) 882-2754. E-mail: jurissonS@missouri.edu. (M.R.L.) Phone: (573) 814-6000 ext 53703. Fax: (573) 814-6551. E-mail: lewismic@missouri.edu.

† Life Sciences Fellowships Program, University of Missouri—Columbia.

‡ Department of Veterinary Medicine and Surgery, University of Missouri—Columbia.

§ Department of Chemistry, University of Missouri—Columbia.

△ Department of Radiology, University of Missouri—Columbia.

⊥ International Institute of Nano and Molecular Medicine, University of Missouri—Columbia.

Nuclear Science and Engineering Institute, University of Missouri—Columbia.

○ Research Service, Harry S. Truman Memorial Veterans' Hospital.

▽ Structural Biology Core, University of Missouri—Columbia.

[a] Abbreviations: SRIF, somatostatin; DTPA, diethylenetriaminepentaacetic acid; octreotide, D-Phe-Cys-Phe-D-Trp-Lys-Thr-Cys-Thr(ol); SSTR, somatostatin receptor; BFC, bifunctional chelate; DOTA, 1,4,7,10-tetraazacyclododecanetetraacetic acid; EDDA/HYNIC, ethylenediamine *N*,*N*′-diacetic acid/hydrazinonicotinic acid; PRRT, peptide receptor radionuclide therapy; SPECT, single photon emission computed tomography; α-MSH, α-melanocyte-stimulating hormone; RC-160, D-Phe-Cys-Tyr-D-Trp-Lys-Val-Cys-Trp-NH_2; Ac-Tyr^3-octreotate, $CH_3C(O)NH$-D-Phe-Cys-Tyr-D-Trp-Lys-Thr-Cys-Thr; LC-ESI-MS, liquid chromatography-electrospray ionization-mass spectrometry; RP-HPLC, reversed-phase HPLC; TOCSY, total correlated spectroscopy; HSQC, heteronuclear single quantum coherence; ($Cys^{4,10}$,D-Phe^7)-α-$MSH_{4–13}$, Ac-Cys-Glu-His-D-Phe-Arg-Trp-Cys-Lys-Pro-Val-NH_2; hsst2, human somatostatin receptor subtype 2; Fmoc, 9-fluorenylmethoxycarbonyl; DSS, 2,2-dimethylsilapentane-5-sulfonic acid; SSTR2, somatostatin receptor subtype 2.

10.1021/jm701056x CCC: $40.75
Published on Web 02/13/2008

Table 1. Octreotide Analogue Sequences and Their Calculated and Observed Molecular Weights by ESI-MS

		linear peptide		disulfide peptide		Re-peptide complex[b]	
peptide	peptide sequence[a]	$(M + H)^+$ calcd	$(M + H)^+$ obsd	$(M + H)^+$ calcd	$(M + H)^+$ obsd (purity, %)	$(M + H)^+$ calcd	$(M + H)^+$ obsd (purity, %)
octreotide	NH_2-DFCFDWKTCT(ol)	1021.5	1021.4	1019.4	1019.5 (99.0)	1220.4	1221.7 (97.7)
Ac-octreotide	Ac-DFCFDWKTCT(ol)	1063.5	1063.3	1061.5	1061.6 (98.8)	1262.4	1263.9 (96.3)
Tyr^3-octreotate	NH_2-DFCYDWKTCTOH	1051.4	1051.5	1049.4	1049.5 (98.6)	1250.4	1251.9 (98.7)
Ac-Tyr^3-octreotate	Ac-DFCYDWKTCTOH	1093.4	1093.4	1091.4	1091.5 (98.4)	1292.4	1293.8 (97.8)
DOTA-Tyr^3-octreotide[c]	DOTA-DFCYDWKTCT(ol)	1423.6	1424.0	1421.6	1421.8 (99.2)	NA[d]	NA[d]

[a] NH_2 and Ac represent *N*-terminal NH_2 and $NHC(O)CH_3$, respectively; (ol) and OH represent *C*-terminal CH_2OH and COOH, respectively. [b] Both ^{185}Re and ^{187}Re peaks were observed. For clarity, values are reported for ^{187}Re, the more abundant isotope. [c] Used as the competitive binding assay standard when radiolabeled with ^{111}In. [d] NA, not applicable.

with decay properties appropriate for targeted radiotherapy. Taking advantage of their affinity for sulfur and nitrogen ligands, Re and Tc radiometals can be added directly into the disulfide bond of SRIF derivatives, using a Cys-S-Re/Tc-S-Cys structure to form the cyclic peptide. Previously, the potential of this integrated radiolabeling approach was demonstrated in studies comparing both BFC and metal cyclization methods to Tc-/Re-labeling of α-melanocyte-stimulating hormone (α-MSH) peptides.[12] Successful integration of the radiometal into the disulfide bond of the α-MSH derivative ($Cys^{3,4,10}$,D-Phe^7)-α-MSH_{3-13} (Ac-Cys-Cys-Glu-His-D-Phe-Arg-Trp-Cys-Lys-Pro-Val-NH_2) resulted in highly stable radiometal−peptide conjugates with the greatest tumor uptake observed for the α-MSH complexes studied.[12,13] Metal cyclization (Re or Tc, whether radiometal or nonradiometal) was shown to result in higher tumor uptake and retention, even for radioiodinated α-MSH analogues.[12,14,15] Increased retention of radioactivity in tumors should translate to improved tumor imaging contrast, as well as more effective therapy at lower doses, sparing the nontarget tissues. Applying this design strategy to SRIF analogues, and potentially improving the status of diagnostic imaging and targeted radiotherapy with SRIF peptide-based radiopharmaceuticals, is therefore attractive.

A limited number of studies have been reported on the Re-/Tc-cyclization of SRIF analogues, describing modest success in receptor binding and tumor uptake. Zamora et al., for example, directly labeled the octreotide analogue RC-160 (D-Phe-Cys-Tyr-D-Trp-Lys-Val-Cys-Trp-NH_2) with ^{188}Re and observed growth inhibition and partial regressions of human prostate tumor xenografts in mice.[16,17] Octreotide cyclized with ^{188}Re selectively localized in small-cell lung cancer lesions of mice, albeit with somewhat lower tumor-to-normal tissue ratios compared to the BFC-radiolabeled octreotide peptide, were also examined.[18] While ^{188}Re-octreotide and ^{188}Re-RC-160 have shown some promise as radiopharmaceutical agents, they have fared no better to date than their iodinated counterparts and have suffered from prolonged retention in the liver, with subsequent slow clearance through the intestines (more renal uptake was observed for ^{188}Re-octreotide).[16,18,19] These disadvantages would likely lead to sizable nontarget tissue doses in addition to causing difficulties in clinical applications for certain tumors (e.g., pancreatic cancer).

The modest performance of the Re-/Tc-cyclized octreotide analogues previously reported may be due to suboptimal peptide sequences rather than to the method of radiometal incorporation; their lipophilic nature is consistent with their tendency to exhibit high hepatobiliary clearance. In several studies employing the BFC-radiolabeling approach, alterations made to the basic octreotide peptide structure yielded complexes with greater hydrophilicities and tumor-targeting properties.[2,8,9] To the best of our knowledge, radiometal cyclization has not been investigated with such "optimized" octreotide peptide derivatives. Therefore, we investigated the structure–activity relationship in a series of octreotide peptides modified at the peptide *N*-terminus, the peptide *C*-terminus, and/or the third amino acid of the peptide sequence. These subtle changes in peptide structure had dramatic effects on the Re(V) coordination sphere, overall Re−peptide complex structure, and SSTR binding affinity. The findings presented herein demonstrate the importance of understanding the consequences of structural modifications when developing metal-peptide complexes for SSTR targeting and offer new insights for future designs.

Results and Discussion

Four reduced linear peptide sequences (octreotide, Ac-octreotide, Tyr^3-octreotate, and Ac-Tyr^3-octreotate, Table 1) were cyclized with nonradioactive Re via transchelation reactions with $[ReOCl_3(OPPh_3)(SMe_2)]$ in aqueous methanol solutions (see the Experimental Section). Analysis of the crude product solutions by liquid chromatography−electrospray ionization−mass spectrometry (LC−ESI−MS) confirmed the expected Re−peptide complex mass for the main product of each reaction. Some of the linear peptide starting material was converted to a Re−free disulfide-bridged peptide that gave rise to a small peak in each of the chromatograms (10–22%, confirmed by both LC−ESI−MS and reversed-phase HPLC (RP−HPLC) coinjection with a synthesized standard). Generation of this side product is not surprising given the basic starting conditions and the single phase nature of this intramolecular reaction (versus the biphasic and intermolecular Re cyclization reaction), both of which can facilitate disulfide formation. Also noteworthy was the observance of another, smaller peak (minor product; 6–12%) with the predicted Re−product mass, yet with a significantly different retention time from the major Re product.

Interestingly, the RP-HPLC elution pattern of the three peptide products formed from each sequence was affected by the *N*-terminus of the linear peptide used in the reaction. For example, Re cyclization with octreotide (*N*-NH_2) resulted in an elution order of minor, disulfide, and major products, whereas a major, disulfide, minor product order was observed under the same RP-HPLC conditions following Re integration into Ac-octreotide. A retention time comparison of the crude product solutions (Table 2) showed that acetylation of the *N*-termini resulted in the preferred formation of products with retention times that were significantly closer to their respective disulfide-bridged peptides, and which always eluted between the two Re−peptide products. These results suggested the involvement of the *N*-terminus in Re complexation and the formation of isomers with different metal coordination spheres. Formation of syn and anti isomers would be expected to give products with similar retention times, but such products were not observed. With several amides and, for the nonacetylated peptides, an unprotected *N*-terminal amine near the metal center,

Table 2. Comparison of RP-HPLC Retention Times of the Re Cyclization Products[a]

linear peptide	retention time (min)		
	disulfide product	major Re product	minor Re product
octreotide	19.6	30.0	17.4
Ac-octreotide	27.6	25.5	30.4
Tyr^3-octreotate	16.1	23.9	14.6
Ac-Tyr^3-octreotate	20.4	19.0	22.6

[a] Values were obtained from analytical RP-HPLC runs using a 35-min linear gradient from 15 to 40% solvent B in solvent A, a 1 mL/min flow rate, and UV detection at 280 nm ($A = 0.1\%$ TFA in H_2O; $B = 0.1\%$ TFA in CH_3CN).

formation of more than one configuration for Re coordination was certainly reasonable.

Therefore, to investigate the role of the peptide *N*-terminus in Re complexation, each of the four nonradioactive Re-cyclized major products was purified by semipreparative RP-HPLC and subsequently lyophilized. The purified major products were characterized by LC−ESI−MS (Table 1), and their solution-phase structures were examined by two-dimensional nuclear magnetic resonance (2D NMR) spectroscopy. The four disulfide-cyclized "parent" peptides (Re−free) were also synthesized, purified by RP-HPLC, confirmed by LC−ESI−MS (Table 1), and analyzed by 2D NMR spectroscopy. Purification was not carried out for the minor Re-cyclized products due to insufficient amounts of material formed during the reactions.

In order to identify the Re(V) coordination spheres, complete ^1H and ^{13}C chemical shift assignments (Tables 3 and 4 and S1−S6 (Supporting Information)) for the Re−peptide complexes and their parent disulfide-bridged peptides were obtained from 2D $^1H-^1H$ total correlated spectroscopy (TOCSY) and $^1H-^{13}C$ heteronuclear single quantum coherence (HSQC) NMR spectra. Natural abundance $^1H-^{13}C$ HSQC NMR experiments were used to detect the backbone carbon chemical shift changes in the Re−peptides versus the parent peptides. Overlays of the spectra for each Re−peptide and its parent peptide showed that most peaks aligned well in the HSQC spectra. However, significant downfield shifts were observed for both the C_α and C_β (e.g., 10.4–15.6 ppm) and the H_α and H_β (e.g., 0.58–1.43 ppm) of Phe^3/Tyr^3 for all four metal-cyclized peptides. In addition, downfield shifts of 10.8–12.4 ppm for the C_α and 1.05–1.08 ppm for the H_α of Thr^6 were observed for the acetylated metal-cyclized peptides, whereas a 9.8–10.5 ppm downfield shift occurred for the C_α of D-Phe^1 for the nonacetylated metal-cyclized peptides. The results indicate that these residues were likely involved in the Re coordination. Chemical shift alterations of Cys^2-βCH_2 and Cys^7-βCH_2 showed that the thiolate sulfurs of Cys^2 and Cys^7 were coordinated to the Re metal center. For example, significant upfield shifts of 4.7–6.5 ppm were observed for C_β of Cys^2 for all four Re-cyclized peptides. Upfield shifts of 2.7–3.8 ppm and downfield shifts of 1.5–2.9 ppm were observed for C_β of Cys^7 for nonacetylated and acetylated metal-cyclized peptides, respectively. In addition, downfield shifts up to 1.12 ppm were observed for H_β for both Cys residues for all four Re-cyclized peptides.

Further analyses were carried out on the 2D TOCSY spectra, which show cross peaks between the backbone amide protons and the side chain protons of each residue. Cross peaks from two backbone amide protons, Phe^3/Tyr^3 and Thr^6, were absent from the TOSCY spectra of the acetylated metal-cyclized peptides (e.g., Figure 1), suggesting these two amide protons had been lost during complexation. Thus, each Re(V) center of the acetylated complexes was coordinated to the two cysteine sulfhydryls (Cys^2 and Cys^7) and the amide nitrogens from both Phe^3/Tyr^3 and Thr^6. In the case of the nonacetylated metal-cyclized peptides, only one amide proton resonance, namely Phe^3/Tyr^3, was absent from the TOCSY spectra. As expected, the *N*-terminal amine was not found on the TOCSY spectra for the parent nonacetylated peptides, due to the fast exchange with bulk water resonance. Interestingly, a single *N*-terminus amine resonance was observed with cross peaks to the side chain protons of D-Phe^1 in the TOCSY spectra of the nonacetylated metal-cyclized peptides. Therefore, in the nonacetylated Re−peptides, each Re(V) center was again coordinated to the two cysteine sulfhydryls and the amide nitrogen from Phe^3/Tyr^3. However, unlike the acetylated Re−peptides, the final coordination site was filled by the *N*-terminal amine (D-Phe^1) rather than a second amide nitrogen. The derived Re(V) coordination spheres are summarized in Table 5.

A single stable conformation was observed in the NMR spectra of the acetylated metal-cyclized peptides (Tables 3 and S1 (Supporting Information)). In further contrast to the acetylated peptides, the *N*-NH_2 peptide complex NMR spectra showed two distinct sets of signals for each peptide, indicating that two isomers existed in solution (Tables S3 and S5, Supporting Information). An integration of NMR peak volumes indicated the presence of approximately 65% and 35% for major and minor isomers, respectively. Each set of peaks identified the same coordination ligands for the Re(V) metal centers, suggesting that these isomers differed from one another in overall structure, but not in complexation to the metal. The Re(V) coordination spheres for complexes of the octreotide sequence, with and without *N*-terminal acetylation, are illustrated in Figure 2, with the Re−free parent peptide shown for comparison.

Disulfide-bridged octreotide (*N*-NH_2) has a large ring of 20 atoms that positions the peptide in the β-turn configuration and is responsible for high-affinity SSTR binding. When octreotide was cyclized with Re, the 17-atom large ring formed was more constrained, leading to perturbations in the structure of the β turn relative to that of the parent peptide. Here, the *N*-terminus coordinated to the metal, forming an eight-membered ring with the basic NH_2 donor in preference to a five- or six-membered ring with one of the amide nitrogen donors that neighbor the cysteine residues. This coordination certainly affected the structure of the peptide near the *N*-terminus but likely did not contribute considerable strain on the pharmacophore-containing ring. Acetylating the *N*-terminus disfavored its coordination to Re and resulted in the amide nitrogen of Thr^6 replacing it in the metal coordination sphere. Consequently, the large ring in the Re−Ac-octreotide consisted of only 11 atoms, which brought the metal center closer to the receptor pharmacophore and further disrupted its configuration relative to the parent peptide. As expected, the same ring sizes were observed for the Tyr^3-octreotate and Ac-Tyr^3-octreotate Re complexes, since the location of the differences between octreotide and Tyr^3-octreotate were not involved in metal cyclization. These results indicated that, due to their proximity to the receptor binding sequence, the Re(V) centers of the metal-peptide complexes may interfere with SSTR binding and that a greater negative effect would be expected for the acetylated Re complexes.

Comparable findings were reported for a Re-cyclized α-MSH peptide containing two Cys residues (Ac-Cys-Glu-His-D-Phe-Arg-Trp-Cys-Lys-Pro-Val-NH_2, ($Cys^{4,10}$,D-Phe^7)-α-MSH_{4-13}).[13] Though the eight amino acid octreotide analogues and the 10 amino acid α-MSH peptide have different sequences and target different receptors, the disulfide- and Re-cyclized peptides have several interesting similarities. The octreotide analogues have

Table 3. ^{1}H and ^{13}C NMR Chemical Shift Assignments[a] of Re−Ac-octreotide

residue	NH	αCH	βCH	others
N-terminus				CH_3: 2.08 (17.7)
D-Phe[1]	8.09	4.50 (50.5)	3.00 (33.9)	δ: 7.27 (126.9); ϵ: 7.37 (126.1); ζ: 7.32 (124.5)
Cys[2]	8.08	4.76[b]	2.83, 3.28 (32.2)	
Phe[3]		5.13 (65.0)	3.68, 4.33 (46.5)	δ: 7.15 (126.4); ϵ: 7.24 (125.8); ζ: 7.20 (124.1)
D-Trp[4]	7.53	4.63 (50.1)	3.18, 3.28 (24.1)	δ1: 7.20 (122.2); ϵ1: 10.14; ϵ3: 7.60 (115.7); ζ2: 7.48 (109.3); ζ3: 7.23 (119.1); η2: 7.19 (116.5)
Lys[5]	8.34	3.78 (50.2)	1.46, 1.64 (24.7)	γ: 1.03 (17.4); δ: 1.55 (22.1); ϵ: 2.90 (35.1); ζ: 7.54
Thr[6]		5.39 (66.6)	4.44 (62.1)	γ2: 1.45 (12.3)
Cys[7]	8.21	4.63 (51.5)	3.49, 3.64 (31.5)	
Thr[8]	7.75	3.82 (52.1)	4.01 (62.0)	γ2: 1.12 (14.8)
C-terminus				CH_2: 3.61, 3.70 (57.1)

[a] Chemical shifts (ppm) were referenced relative to DSS and were measured at 25 °C. ^{1}H chemical shift values are listed with ^{13}C values in parentheses. The chemical shifts are generally accurate to 0.02 ppm for ^{1}H and 0.1 ppm for ^{13}C. [b] The chemical shift of $^{13}C_\alpha$ could not be assigned due to overlapping resonance with H_2O in the $^{1}H-^{13}C$ HSQC spectrum.

Table 4. ^{1}H and ^{13}C NMR Chemical Shift Assignments[a] of Disulfide-Cyclized Ac-octreotide

residue	NH	αCH	βCH	others
N-terminus				CH_3: 2.00 (17.6)
D-Phe[1]	8.24	4.59 (51.1)	3.04 (33.2)	δ: 7.27 (126.6); ϵ: 7.38 (126.1); ζ: 7.34 (124.6)
Cys[2]	8.16	4.69[b]	2.86, 2.72 (37.2)	
Phe[3]	8.20	4.66 (50.8)	2.93, 3.04 (34.1)	δ: 7.24 (126.7); ϵ: 7.36 (126.1); ζ: 7.37 (124.6)
D-Trp[4]	8.63	4.32 (51.7)	2.92, 3.04 (22.0)	δ1: 7.14 (121.9); ϵ1: 10.20; ϵ3: 7.58 (115.7); ζ2: 7.51 (109.3); ζ3: 7.26 (119.3); η2: 7.20 (116.7)
Lys[5]	8.33	3.89 (50.2)	1.29, 1.58 (25.4)	γ: 0.39, 0.56 (17.3); δ: 1.32 (22.0); ϵ: 2.70 (35.0); ζ: 7.48
Thr[6]	7.99	4.31 (55.8)	4.37 (62.5)	γ2: 1.24 (15.0)
Cys[7]	8.02	4.80[b]	2.94, 3.19 (35.3)	
Thr[8]	7.72	3.86 (52.4)	4.02 (62.0)	γ2: 1.16 (14.8)
C-terminus				CH_2: 3.63, 3.72 (57.1)

[a] Chemical shifts (ppm) were referenced relative to DSS and were measured at 25 °C. ^{1}H chemical shift values are listed with ^{13}C values in parentheses. The chemical shifts are generally accurate to 0.01 ppm for ^{1}H and 0.1 ppm for ^{13}C. [b] Chemical shifts of $^{13}C_\alpha$ could not be assigned due to overlapping resonances with H_2O in the $^{1}H-^{13}C$ HSQC spectrum.

a four amino acid receptor pharmacophore (Phe[3]/Tyr[3]-D-Trp[4]-Lys[5]-Thr[6]) immediately bordered by two Cys residues. The α-MSH peptide also has a four amino acid receptor binding sequence (His[6]-D-Phe[7]-Arg[8]-Trp[9]) between two flanking Cys residues, yet with an additional amino acid (Glu[5]) between Cys[4] and the binding sequence. This extra amino acid resulted in a 23-membered ring for the Re−free cyclic peptide, three atoms larger in size than the disulfide-cyclized octreotide analogues. Upon coordination of Re, however, the ring size was reduced from 23 atoms to 18 atoms (a 22% decrease). As described above, the octreotide analogues rings were reduced in size as well, from 20 atoms for the parent disulfide peptides to either 17 atoms (a 15% decrease) or 11 atoms (a 45% decrease) for the nonacetylated and acetylated peptides, respectively. Furthermore, in each of the Re−peptide complexes, one or more of the binding sequence amino acids was involved in coordination to the metal; Trp[9] for Re-(Cys[4,10],D-Phe[7])-α-MSH_{4-13}, Phe[3]/Tyr[3] for the nonacetylated Re−octreotide analogues, and Phe[3]/Tyr[3] and Thr[6] for the acetylated Re−octreotide analogues. For the (Cys[4,10],D-Phe[7])-α-MSH_{4-13} peptide, direct metal cyclization resulted in nearly a 100-fold reduction in receptor affinity relative to its disulfide-cyclized counterpart. This loss of binding affinity was attributed to both the proximity of the Re-coordination sphere to the receptor binding amino acids and to the involvement of Trp[9] in metal binding.

Consequently, to determine the extent of the effect on receptor binding caused by integration of the metal center, SSTR binding affinity values were obtained for the Re-cyclized peptide series and were correlated to the NMR structural findings. The concentrations of peptides that caused half-maximal inhibition (IC_{50} values) of ^{111}In-DOTA-Tyr[3]-octreotide binding to AR42J rat pancreatic carcinoma cells are shown in Table 5. Each of the Re−peptide complexes was found to target the receptor; IC_{50} values ranged from 29 to 636 nM, and the associated receptor binding affinities were in the following order: Re−Ac-octreotide < Re−octreotide < Re−Ac-Tyr[3]-octreotate < Re−Tyr[3]-octreotate. Reubi et al.[20] reported IC_{50} values for the human somatostatin receptor subtype 2 (hsst2) of 22 and 11 nM, respectively, for In-DTPA-octreotide and Y-DOTA-Tyr[3]-octreotide, the nonradioactive forms of two of the most characterized clinical PRRT agents. Therefore, the 29 nM IC_{50} value for Re−Tyr[3]-octreotate, the highest affinity complex of the present study, demonstrated the potential of the direct metal cyclization approach in designing SRIF analogues with reasonable in vitro SSTR targeting.

The magnitude and order of the IC_{50} values correlated well with the NMR data. First, all of the Re−peptide spectra showed shifted ^{1}H and ^{13}C NMR signals of the receptor pharmacophore residues, suggesting differences in the structure and/or the electronic environment of the β turns with respect to their parent disulfide peptides. Such changes are consistent with the somewhat elevated IC_{50} values observed for the series (target IC_{50} range is 1–30 nM) and suggest that modifications made to reduce or eliminate these differences may improve SSTR affinity. Second, the acetylated peptide analogues showed lower receptor affinities (higher values) than their counterparts with amine *N*-termini. The NMR data also agreed with this outcome, showing that the metal centers of the *N*-acetylated peptide complexes actually coordinated to two amino acids of the receptor binding sequence, namely the amide nitrogens of Phe[3]/Tyr[3] and Thr[6]. Furthermore, as observed by others in the field,[2,8,20] the Tyr[3]-octreotate analogues bound to the receptor with a higher affinity than their octreotide counterparts. Further NMR characterization of the Re-cyclized peptides by full three-dimensional structure analysis is currently underway.

These findings may shed light on the less than ideal outcomes previously published for ^{188}Re/^{99m}Tc-cyclized octreotide analogues.[18,21] We have shown that ^{99m}Tc−Tyr[3]-octreotate and

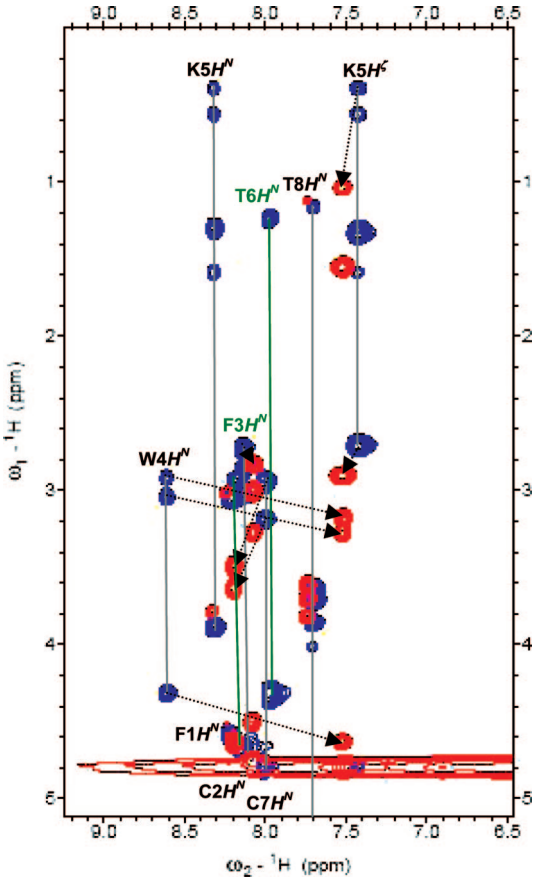

Figure 1. Overlay of 2D $^{1}H-^{1}H$ TOCSY NMR spectra of Re−Ac-octreotide (red) and disulfide-cyclized Ac-octreotide (blue). As indicated by the arrows shown, many proton peaks are shifted upon integration of the Re(V) core into the Ac-octreotide peptide structure. Also, the amide protons of Phe^3 and Thr^6 are missing from the Re−Ac-octreotide spectrum (the corresponding disulfide-cyclized Ac-octreotide protons are labeled in green).

Table 5. Re-Cyclized Peptide Complex Coordination Sites and Somatostatin Receptor Binding Affinities (AR42J Cells)

Re−peptide complex	Re coordination Sites[a]	IC_{50} values (nM)[b]
Re−octreotide	DPhe^1 NH_2	328 ± 65
	Cys^2 sulfhydryl	
	Phe^3 *N*-amide	
	Cys^7 sulfhydryl	
Re−Ac-octreotide	Cys^2 sulfhydryl	637 ± 125
	Phe^3 *N*-amide	
	Thr^6 *N*-amide	
	Cys^7 sulfhydryl	
Re−Tyr^3-octreotate	DPhe^1 NH_2	29.2 ± 6.1
	Cys^2 sulfhydryl	
	Tyr^3 *N*-amide	
	Cys^7 sulfhydryl	
Re−Ac-Tyr^3-octreotate	Cys^2 sulfhydryl	106 ± 12
	Tyr^3 *N*-amide	
	Thr^6 *N*-amide	
	Cys^7 sulfhydryl	

[a] Re(V) metal coordination sites were assigned from 2D $^{1}H-^{1}H$ TOCSY and $^{1}H-^{13}C$ HSQC NMR data analysis. [b] IC_{50} values were determined from competitive binding assays with ^{111}In-DOTA-Tyr^3-octreotide in AR42J cells and are presented as average ± SEM from triplicate measurements.

nonradioactive Re−Tyr^3-octreotate coelute following RP-HPLC coinjection, suggesting similar structures at the macroscopic and radiotracer levels.[21] It is therefore reasonable to assume a similar coordination scheme for ^{188}Re−octreotide as for the nonradioactive Re−octreotide complex reported herein. Hence, both ^{188}Re−octreotide and ^{99m}Tc−Tyr^3-octreotate would be expected to have perturbed SSTR pharmacophore structures compared not only to their disulfide-cyclized parent peptides, but also to octreotide derivatives radiolabeled at locations remote to the receptor binding sequence (e.g., BFC-radiolabeled analogues). We also reported in vitro instability of ^{99m}Tc-Tyr^3-octreotate in phosphate-buffered saline at pH 7.4 and 37 °C (physiologic conditions) and in vivo evidence supporting the oxidation and loss of the ^{99m}Tc(V) center from the radiotracer to generate pertechnetate ($^{99m}TcO_4^-$).[21] Formation of an eight-membered ring through binding of the *N*-terminal amine to the ^{99m}Tc, as described above for Re−Tyr^3-octreotate, may have resulted in loose coordination of the amine and vulnerability of the ^{99m}Tc(V) metal center toward oxidation. Since Re is more easily oxidized than Tc, similar ^{188}Re-cyclized octreotide analogues may also be expected to suffer instability at the radiotracer level. Taken together, the likely reduced affinity for SSTR binding and instability of the radiopeptide complex may explain the observed lower tumor-to-normal tissue ratios, higher background activity, and slower clearance of ^{188}Re−octreotide[18] relative to the octreotide radiotracer in which the radiometal was incorporated via a bifunctional chelating moiety.

An improved integrated radiolabeling design, in which the metal center is distanced from the SSTR pharmacophore, may increase receptor binding, tumor uptake and retention, and improve clearance properties of Re- and Tc-cyclized octreotide analogues. The potential for such a design improvement was reported for α-MSH peptide analogues by Giblin et al.[13] In this work, direct metalation into the disulfide bond of a peptide containing two cysteine residues resulted in a cyclic structure with lower receptor binding than the disulfide-cyclized analogue (metal coordination had interfered with receptor binding). The addition of a third Cys residue at the *N*-terminus yielded radiometalated derivatives with very high and specific receptor binding, high tumor uptake, and longer tumor residence times. The Tc- or Re-coordinated to three Cys sulfhydryls and one Cys amide, presumably distancing the metal coordination from the binding pharmacophore and restoring receptor affinity. Applying this strategy to Re- and Tc-cyclized octreotide analogues may also lead to a more tightly bound metal center and increased stability at the radiotracer level. A new generation of SSTR-targeting peptides, incorporating a third cysteine residue into the octreotide sequences, is currently under investigation.

Conclusions

A series of Re-cyclized octreotide derivatives was synthesized, assessed for their somatostatin receptor targeting abilities and structurally compared against their disulfide-cyclized parent peptides. Integrating a nonradioactive Re(V) metal into the disulfide bond of these octreotide analogues resulted in low SSTR binding affinities, likely due to perturbation of the peptide β turn relative to the metal-free parent structure. Altering the *N*-terminus of these peptides had a significant effect on the Re(V) coordination sphere, overall peptide structure, and SSTR binding affinity. The SSTR binding was disrupted to a greater degree in the *N*-acetylated peptides, where the Re(V) centers were in closer proximity to the β turns than in the *N*-NH_2 peptides, where coordination to the *N*-terminal amine moved the Re centers away from the SSTR binding sequence. These studies demonstrated the importance of understanding the structure–activity relationships of metal-cyclized Re/Tc-octreotide complexes and helped explain the shortcomings of complexes of this type in studies reported to date. The data

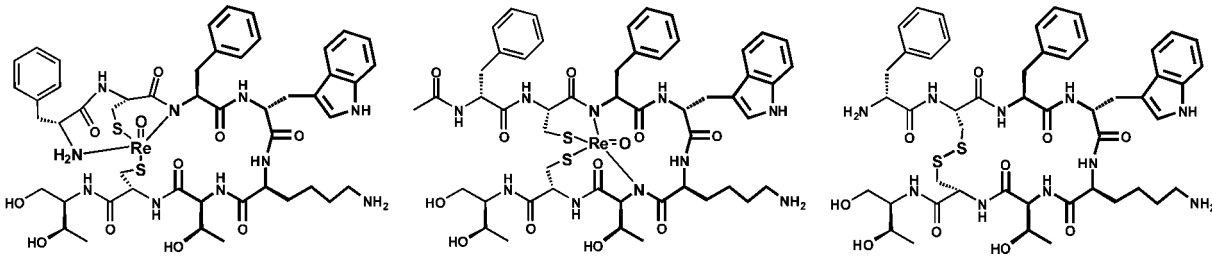

Figure 2. Structures of Re−octreotide (left) and Re−Ac-octreotide (middle) with somatostatin pharmacophore sequences shown in bold. Disulfide-cyclized octreotide is shown (right) for comparison.

suggest that structural modifications to distance the Re/Tc coordination sphere from the SSTR pharmacophore may lead to new radiopharmaceutical agents with enhanced receptor binding and improved radiopharmaceutical properties.

Experimental Section

General Methods. Reagents and solvents were purchased from VWR Scientific Products (St. Louis, MO), Novabiochem (San Diego, CA), Fluka (Milwaukee, WI), Macrocyclics (Dallas, TX), and Fischer Scientific (Pittsburgh, PA). All reagents and solvents were HPLC grade, peptide synthesis grade, or of the highest purity obtainable and were used without further purification.

Reversed-phase HPLC (RP-HPLC) analysis and semipreparative purification were carried out on a Beckmann Coulter System Gold HPLC equipped with a 168 diode array detector, a 507e autoinjector, and the 32 KARAT software package (Beckmann Coulter, Fullerton, CA). Analytical HPLC was performed on a Grace Vydac (Hesperia, CA) Protein & Peptide C18 column (300 Å, 0.46 cm × 25 cm, 5 μm), or a Keystone Scientific, Inc. (Bellefonte, PA) C-18 Kromasil column (100 Å, 0.46 × 15 cm, 5 μm) with linear gradients of solvent B in solvent A (A = 0.1% TFA in water; B = 0.1% TFA in acetonitrile), a 1 mL/min flow rate, and UV detection at 214 and 280 nm. Semipreparative RP-HPLC was performed on a Waters (Milford, MA) Prep Nova-Pak HR C18 column (60 Å, 1.9 cm × 30 cm, 6 μm), also using linear gradients of solvent B in solvent A, but with flow rates up to 10 mL/min and UV detection at 225 and 280 nm. Liquid chromatography−electrospray ionization−mass spectrometry (LC−ESI−MS) analyses were carried out on a Thermo Finnigan LC system consisting of a P4000 quaternary LC pump and SCM1000 vacuum degasser, an AS3000 autosampler, and a UV6000LP diode-array detector connected to a Thermo Finnigan TSQ7000 triple-quadrupole mass spectrometer (Thermo Finnigan, San Jose, CA). A Waters Nova-Pak C18 column (60 Å, 0.39 × 30 cm, 4 μm) was used for the LC−ESI−MS experiments.

Synthesis and Purification of Parent Peptides. The reduced form "linear" peptides (Table 1) were synthesized with the Advanced ChemTech (Louisville, KY) 396 Omega multiple peptide synthesizer, using standard solid-phase 9-fluorenylmethoxycarbonyl (Fmoc) chemistry. Each Fmoc amino acid was coupled at least twice. To prepare the linear DOTA-Tyr^3-octreotide peptide, a tris(tertiary butyl ester)-protected DOTA building block was used in the final coupling step. Cleavage and side chain deprotection were achieved by treating the resin with a trifluoroacetic acid solution containing 2.5% each of thioanisole, phenol, water, ethanedithiol, and triisopropylsilane. The crude peptides obtained were characterized by HPLC and LC-MS and were purified by semipreparative HPLC using an in-house optimized multistep gradient.

The disulfide-cyclized "parent" peptides, along with disulfide-bridged DOTA-Tyr^3-octreotide (for IC_{50} experiments below), were prepared by adding 2.8 mL of a 1:1 water/acetonitrile (v/v) solution, 8.5 mL of 0.2 M ammonium acetate, and 1.7 mL of dimethyl sulfoxide to 13 mg of the linear peptides. The 1 mg/mL peptide mixtures were shaken overnight, resulting in near quantitative yields of the disulfide-cyclized peptides. The products were isolated with semipreparative RP-HPLC, characterized by LC−ESI−MS (Table 1), and subsequently lyophilized. Each peptide had a purity of >98%.

Synthesis and Purification of Rhenium−Peptide Complexes. The syntheses of the Re(V) cyclic complexes were achieved via transchelation reactions utilizing modified literature procedures.[13,22] In general, a linear peptide (5–15 mg) was dissolved in an aqueous MeOH solution (62–75%) and the pH was adjusted to 8–9 with 1 N NaOH. Addition of 1.5 mol equiv of the Re(V) complex [$ReOCl_3(OPPh_3)(SMe_2)$], prepared as previously described,[23] resulted in a mint green suspension that, with heating at 65–70 °C for 1 h, gradually cleared to give a brown-orange solution and a gray-black precipitate. After filtration of the crude reaction mixture, semipreparative RP-HPLC separation of the filtrate was employed to isolate the desired Re-cyclized peptide, and the purity and mass of the purified product were verified by LC−ESI−MS (Table 1). Each Re−peptide complex had a purity of >95%.

NMR Studies. NMR spectra were collected on a Varian Unity Inova 600 MHz spectrometer equipped with a 5 mm [^{1}H, ^{15}N, ^{13}C] triple-resonance cold probe. NMR experiments, 2D ^{1}H−^{1}H total correlated spectroscopy (TOCSY) (80 ms mixing time), and ^{1}H−^{13}C heteronuclear single quantum coherence (HSQC), were performed for peptide solution samples. The ^{1}H and ^{13}C chemical shifts were measured at 25 °C from samples in 9:1 H_2O/D_2O, with concentrations ranging from 0.8 to 1.4 mM in 400 μL for Re-cyclized peptides and from 4.2 to 4.5 mM in 600 μL for the parent peptides (e.g., Tables 3 and 4 for Re−Ac-octreotide and Ac-octreotide, respectively; other NMR data tables, Tables S1−S6, are given in the Supporting Information). Re-cyclized complex samples were prepared in SHIGEMI NMR tubes (Shigemi Co., Japan), while the standard NMR tubes were used for the disulfide samples. The pH values of the NMR samples ranged from 2.4 to 4.5. NMR data were processed with NMRPipe[24] and analyzed in SPARKY (Goddard, T.D. and Kneller, D.G., SPARKY3, University of California, San Francisco). Indirect dimensions were normally extended by linear prediction and zero-filled prior to Fourier transformation, and only spectral regions containing signals were retained. The ^{1}H and ^{13}C chemical shifts were referenced to 2,2-dimethylsilapentane-5-sulfonic acid (DSS) as an external standard.[25]

[^{111}In-DOTA]Tyr^3-octreotide. $^{111}InCl_3$ was obtained from Mallinckrodt Medical (St. Louis, MO). The radiolabeling of DOTA-Tyr^3-octreotide was carried out following a modified literature procedure.[26] To 100 μL of a 30 mM sodium acetate/25 mM sodium ascorbate solution (pH = 5.0) were added 50 μL of $^{111}InCl_3$ and 1 μg of disulfide-cyclized DOTA-Tyr^3-octreotide, and the mixture was heated for 30 min at 99 °C. The ^{111}In-DOTA-Tyr^3-octreotide was purified by RP-HPLC using a 1 mL/min flow rate through a Phenomenex Jupiter (Torrance, CA) C18 column (300Å, 0.46 cm × 25 cm, 5 μm) with a 0–50% linear gradient of solvent B in solvent A over 30 min and UV absorbance monitored at 214 and 280 nm. RP-HPLC coinjection of the purified product with ^{nat}In-DOTA-Tyr^3-octreotide gave a single radioactive peak that coeluted with the UV peak of the nonradioactive standard.

Cell Culture. AR42J rat pancreatic carcinoma cells, known to express the somatostatin receptor subtype 2 (SSTR2), were obtained from the American type Culture Collection (Manassas, VA) and initially maintained by the Cell and Immunobiology Core Facility at the University of Missouri-Columbia. Monolayer cell cultures were maintained by serial passage in exponential growth phase in RPMI 1640 medium (GIBCO-Invitrogen, Carlsbad, CA), supplemented with 10% fetal bovine serum, 2 mM L-glutamine, and 48

μg/mL gentamycin, in a humidified atmosphere of 5% CO_2/air at 37 °C. Cell viability was determined to be >98% by trypan blue exclusion and hemacytometry. Prior to cell experiments, the growth media was removed and the cells were gently washed with Ca^{2+}/Mg^{2+}-free phosphate-buffered saline. Following removal of the phosphate-buffered saline, the cells were typsinized with 5 mL of TrypLE Express (GIBCO-Invitrogen, Carlsbad, CA). Trypsin was quenched by the addition of complete medium (RPMI 1640 Medium (Custom), GIBCO-Invitrogen, Carlsbad, CA, supplemented with 10–20% fetal bovine serum). The cells were collected by centrifugation, the supernatant was removed, and the cells were resuspended in complete medium and counted.

IC_{50} Cell Studies. The in vitro somatostatin receptor binding affinities of the Re-cyclized peptides were determined from competitive binding assays with ^{111}In-DOTA-Tyr^3-octreotide in AR42J rat pancreatic tumor cells. The procedures used in these studies were based on methods reported by Smith et al.[27] Briefly, trypsinized SSTR2-expressing cells were suspended in fresh media at a concentration of 1×10^7 cells/mL. Triplicate aliquots of cells (2×10^6 cells/assay) were incubated at 37 °C in a shaking water bath with a fixed quantity of ^{111}In-DOTA-Tyr^3-octreotide (0.2 μCi/assay) and various concentrations of the Re−peptide complexes (ranging from 10^{-5} to 10^{-10} M). After 2 h, the cell-bound radioactivity was separated by centrifugation (1 min at 10,000 rpm), the incubation medium was aspirated, and the cell pellet was subsequently cooled on an ice block and washed three times with fresh 4 °C media. The amount of ^{111}In-DOTA-Tyr^3-octreotide bound to the cells was determined by measuring the radioactivity of the cell pellets on a Wallac 1480 Wizard 3″ automated gamma counter (PerkinElmer Life Sciences, Gaithersburg, MD). The percent of cell-bound radioactivity versus the Re-cyclized peptide concentration was plotted and analyzed using GraFit software (Version 4.0.10, Erithacus Software Ltd., Horley, Surrey, UK). The concentration of Re−peptide ligands that caused half-maximal inhibition (IC_{50} values) of ^{111}In-DOTA-Tyr^3-octreotide binding are listed in Table 5.

Acknowledgment. We thank Whitney Wells for technical assistance. This research was supported through a University of Missouri Life Sciences Postdoctoral Fellowship (H.M.B.-H.), by NIH Grant Nos. DHHS1 F32 CA119894 (H.M.B.-H.) and DHHS1 P50 CA103130 (S.S.J. and M.R.L.; WA Volkert, PI), and by DOE Grant No. DE-FG02-01ER63192 (S.S.J.). We acknowledge the Department of Veterans Affairs for providing resources and use of facilities at the Harry S. Truman Memorial Veterans' Hospital in Columbia, MO.

Supporting Information Available: ^{1}H and ^{13}C NMR chemical shift tables (Tables S1−S6) for Re- and disulfide-cyclized Ac-Tyr^3-octreotate, octreotide, and Tyr^3-octreotate. This material is available free of charge via the Internet at http://pubs.acs.org.

References

(1) Van Essen, M.; Krenning Eric, P.; de Jong, M.; Valkema, R.; Kwekkeboom Dik, J. Peptide Receptor Radionuclide Therapy with Radiolabelled Somatostatin Analogues in Patients with Somatostatin Receptor Positive Tumours. *Acta Oncol.* **2007**, *46*, 723–734.

(2) de Jong, M.; Breeman, W. A. P.; Bakker, W. H.; Kooij, P. P. M.; Bernard, B. F.; Hofland, L. J.; Visser, T. J.; Srinivasan, A.; Schmidt, M. A.; Erion, J. L.; Bugaj, J. E.; Macke, H. R.; Krenning, E. P. Comparison of ^{111}In-Labeled Somatostatin Analogs for Tumor Scintigraphy and Radionuclide Therapy. *Cancer Res.* **1998**, *58*, 437–441.

(3) de Jong, M.; Bakker, W. H.; Krenning, E. P.; Breeman, W. A. P.; van der Pluijm, M. E.; Bernard, B. F.; Visser, T. J.; Jermann, E.; Behe, M.; Powell, P.; Macke, H. R. Yttrium-90 and Indium-111 Labeling, Receptor Binding and Biodistribution of [DOTA^0,D-Phe^1,Tyr^3]Octreotide, a Promising Somatostatin Analog for Radionuclide Therapy. *Eur. J. Nucl. Med.* **1997**, *24*, 368–371.

(4) Heppeler, A.; Froidevaux, S.; Macke, H. R.; Jermann, E.; Behe, M.; Powell, P.; Hennig, M. Radiometal-Labelled Macrocyclic Chelator-Derivatized Somatostatin Analogue with Superb Tumour-Targeting Properties and Potential for Receptor-Mediated Internal Radiotherapy. *Chem.−Eur. J.* **1999**, *5*, 1974–1981.

(5) Lewis, J. S.; Wang, M.; Laforest, R.; Wang, F.; Erion, J. L.; Bugaj, J. E.; Srinivasan, A.; Anderson, C. J. Toxicity and Dosimetry of ^{177}Lu-DOTA-Y3-Octreotate in a Rat Model. *Int. J. Cancer* **2001**, *94*, 873–877.

(6) Kwekkeboom, D. J.; Bakker, W. H.; Kooij, P. P. M.; Konijnenberg, M. W.; Srinivasan, A.; Erion, J. L.; Schmidt, M. A.; Bugaj, J. L.; de Jong, M.; Krenning, E. P. [^{177}Lu-DOTA^0,Tyr^3]Octreotate: Comparison with [^{111}In-DTPA^0]Octreotide in Patients. *Eur. J. Nucl. Med.* **2001**, *28*, 1319–1325.

(7) Anderson, C. J.; Dehdashti, F.; Cutler, P. D.; Schwarz, S. W.; Laforest, R.; Bass, L. A.; Lewis, J. S.; McCarthy, D. W. ^{64}Cu-TETA-Octreotide as a PET Imaging Agent for Patients with Neuroendocrine Tumors. *J. Nucl. Med.* **2001**, *42*, 213–221.

(8) Lewis, J. S.; Lewis, M. R.; Srinivasan, A.; Schmidt, M. A.; Wang, J.; Anderson, C. J. Comparison of Four ^{64}Cu-Labeled Somatostatin Analogs in Vitro and in a Tumor-Bearing Rat Model: Evaluation of New Derivatives for Positron Emission Tomography Imaging and Targeted Radiotherapy. *J. Med. Chem.* **1999**, *42*, 1341–1347.

(9) Lewis, J. S.; Srinivasan, A.; Schmidt, M. A.; Anderson, C. J. In Vitro and in Vivo Evaluation of ^{64}Cu-TETA-Tyr^3-Octreotate. A New Somatostatin Analog with Improved Target Tissue Uptake. *Nucl. Med. Biol.* **1999**, *26*, 267–273.

(10) Decristoforo, C.; Mather, S. J.; Cholewinski, W.; Donnemiller, E.; Riccabona, G.; Moncayo, R. ^{99m}Tc-EDDA/HYNIC-TOC: A New ^{99m}Tc-Labelled Radiopharmaceutical for Imaging Somatostatin Receptor-Positive Tumours: First Clinical Results and Intra-Patient Comparison with ^{111}In-Labelled Octreotide Derivatives. *Eur. J. Nucl. Med.* **2000**, *27*, 1318–1325.

(11) Gabriel, M.; Decristoforo, C.; Donnemiller, E.; Ulmer, H.; Rychlinski, C. W.; Mather, S. J.; Moncayo, R. An Intrapatient Comparison of ^{99m}Tc-EDDA/HYNIC-TOC with ^{111}In-DTPA-Octreotide for Diagnosis of Somatostatin Receptor-Expressing Tumors. *J. Nucl. Med.* **2003**, *44*, 708–716.

(12) Chen, J.; Cheng, Z.; Hoffman, T. J.; Jurisson, S. S.; Quinn, T. P. Melanoma-Targeting Properties of ^{99m}Technetium-Labeled Cyclic α-Melanocyte-Stimulating Hormone Peptide Analogues. *Cancer Res.* **2000**, *60*, 5649–5658.

(13) Giblin, M. F.; Wang, N.; Hoffman, T. J.; Jurisson, S. S.; Quinn, T. P. Design and Characterization of α-Melanotropin Peptide Analogs Cyclized through Rhenium and Technetium Metal Coordination. *Proc. Natl. Acad. Sci. U.S.A.* **1998**, *95*, 12814–12818.

(14) Chen, J.; Cheng, Z.; Owen, N. K.; Hoffman, T. J.; Miao, Y.; Jurisson, S. S.; Quinn, T. P. Evaluation of an ^{111}In-DOTA-Rhenium Cyclized Alpha-MSH Analog: A Novel Cyclic-Peptide Analog with Improved Tumor-Targeting Properties. *J. Nucl. Med.* **2001**, *42*, 1847–1855.

(15) Cheng, Z.; Chen, J.; Quinn, T. P.; Jurisson, S. S. Radioiodination of Rhenium Cyclized α-Melanocyte-Stimulating Hormone Resulting in Enhanced Radioactivity Localization and Retention in Melanoma. *Cancer Res.* **2004**, *64*, 1411–1418.

(16) Zamora, P. O.; Gulhke, S.; Bender, H.; Diekmann, D.; Rhodes, B. A.; Biersack, H.-J.; Knapp, F. F. Jr. Experimental Radiotherapy of Receptor-Positive Human Prostate Adenocarcinoma with ^{188}Re-RC-160, a Directly-Radiolabeled Somatostatin Analog. *Int. J. Cancer* **1996**, *65*, 214–220.

(17) Zamora, P. O.; Bender, H.; Knapp, F. F. Jr.; Biersack, H. J. Radiotherapy of Intrathoracic Carcinoma Xenografts with ^{188}Re-RC-160, a Somatostatin Analog. *Tumor Targeting* **1996**, *2*, 49–59.

(18) Hosono, M.; Hosono, M. N.; Haberberger, T.; Zamora, P. O.; Guhlke, S.; Bender, H.; Knapp, F. F. R.; Biersack, H. J. Localization of Small-Cell Lung Cancer Xenografts with Iodine-125-, Indium-111-, and Rhenium-188-Somatostatin Analogs. *Jpn. J. Cancer Res.* **1996**, *87*, 995–1000.

(19) Haberberger, T.; Zamora, P.; Hosono, M.; Hosono, M. N.; Bender, H.; Guhlke, S.; Knapp, F. F.; Biersack, H. J. Initial Studies on ^{99m}Tc- and ^{188}Re-Somatostatin Analogues: Stannous-Mediated Direct-Labelling and Biodistribution in Normal Mice. In *Technetium, Rhenium and Other Metals in Chemistry and Nuclear Medicine*; Nicolini, M., Mazzi, U., Eds.; SGE Editoriali: Padova, Italy. 1995; *Vol. 4*, 367−372.

(20) Reubi, J. C.; Schar, J.-C.; Waser, B.; Wenger, S.; Heppeler, A.; Schmitt, J. S.; Macke, H. R. Affinity Profiles for Human Somatostatin Receptor Subtypes SST1-SST5 of Somatostatin Radiotracers Selected for Scintigraphic and Radiotherapeutic Use. *Eur. J. Nucl. Med.* **2000**, *27*, 273–282.

(21) Bigott, H. M.; Dannoon, S. F.; Figueroa, S. D.; Hoffman, T. J.; Jurisson, S. S.; Lewis, M. R. Biodistribution and Imaging Studies of Somatostatin Receptors Using Technetium-99m-Cyclized Tyrosine-3-Octreotate. In *Technetium, Rhenium and Other Metals in Chemistry and Nuclear Medicine*, Mazzi, U., Ed.; SGE Editoriali: Padova, Italy, 2006; Vol. 7, pp 295–300.

(22) Giblin, M. F.; Jurisson, S. S.; Quinn, T. P. Synthesis and Characterization of Rhenium-Complexed α-Melanotropin Analogs. *Bioconjugate Chem.* **1997**, *8*, 347–353.

(23) Grove, D. E.; Wilkinson, G. Oxo-Complexes of Rhenium(V). *J. Chem. Soc., A, Inorg. Phys. Theoret.* **1966**, *1224*, 1230.

(24) Delaglio, F.; Grzesiek, S.; Vuister, G. W.; Zhu, G.; Pfeifer, J.; Bax, A. NMRPipe: A Multidimensional Spectral Processing System Based on UNIX Pipes. *J. Biomol. NMR* **1995**, *6*, 277–293.

(25) Wishart, D. S.; Bigam, C. G.; Yao, J.; Abildgaard, F.; Dyson, H. J.; Oldfield, E.; Markley, J. L.; Sykes, B. D. ^{1}H, ^{13}C and ^{15}N Chemical Shift Referencing in Biomolecular NMR. *J. Biomol. NMR* **1995**, *6*, 135–140.

(26) Breeman, W. A. P.; de Jong, M.; Visser, T. J.; Erion, J. L.; Krenning, E. P. Optimizing Conditions for Radiolabeling of DOTA-Peptides with ^{90}Y, ^{111}In and ^{177}Lu at High Specific Activities. *Eur. J. Nucl. Med. Mol. Imaging* **2003**, *30*, 917–920.

(27) Smith, C. J.; Gali, H.; Sieckman, G. L.; Higginbotham, C.; Volkert, W. A.; Hoffman, T. J. Radiochemical Investigations of ^{99m}Tc-N_3S-X-BBN[7–14]NH_2: An in Vitro/in Vivo Structure-Activity Relationship Study Where $X = 0$-, 3-, 5-, 8-, and 11-Carbon Tethering Moieties. *Bioconjugate Chem.* **2003**, *14*, 93–102.

JM701056X